Journal of Solid State Chemistry 182 (2009) 1003–1008

Contents lists available at ScienceDirect

Journal of Solid State Chemistry

journal homepage: www.elsevier.com/locate/jssc

Facile fabrication of rutile monolayer films consisting of well crystalline nanorods by following an IL-assisted hydrothermal route

Peng Peng [a,b,*], Xiaodi Liu [a], Chuansheng Sun [a], Jianmin Ma [a], Wenjun Zheng [a]

[a] Department of Material Chemistry, College of Chemistry, Nankai University, Tianjin 300071, China
[b] Department of Chemistry, Zhoukou Normal University, Zhoukou, Henan 466001, China

ARTICLE INFO

Article history:
Received 22 August 2008
Received in revised form
29 December 2008
Accepted 1 January 2009
Available online 13 January 2009

Keywords:
TiO_2
Rutile
Nanorods films
Ionic liquid

ABSTRACT

In this study, rutile films consisting of rectangular nanorods were facilely deposited on glass substrates from strongly acid solution of $TiCl_4$. The highly ordered array of nanorods was realized in presence of ionic liquid (IL) of [Bmim]Br by following a hydrothermal process. In this process, Degussa P25 nanoparticles served as seeds that were pre-deposited on the substrates to facilitate the array of rutile nanorods. X-ray diffraction (XRD), scanning electron microscopy (SEM), transmission electron microscopy (TEM), and Raman spectrum were used to characterize the obtained nanorod films. The measurements showed that the nanorods were rectangular with width of 100–200 nm and length of more than 1 μm, and grew up typically along *c*-axis to form the arrays against the substrate. The presence of IL was found vital for the formation of rutile nanorods, and the suitable molar ratio of [Bmim]Br to $TiCl_4$ ranged from 500:1 to 1500:1. The excessive [Bmim]Br may hinder the precipitation of rutile particles.

1. Introduction

Titanium dioxide is a versatile material and has been investigated considerably due to its unique optoelectronic and photochemical properties, such as high refractive index, high dielectric constant, and excellent optical transmittance in the visible and near-IR region as well as high performance photocatalysis for water splitting and for degradation of organics [1,2]. Each phase of TiO_2 (anatase, rutile, brookite) presents different physical and chemical properties with different functionalities. In recent years, rutile nanostructure has received increasing attention because it has been demonstrated comparable to anatase in application to photocatalysis, dye-sensitized solar cells (DSCs) and so on [3–6]. However, the synthesis of rutile nanostructures usually requires time-consuming reactions at elevating temperature, even via hydrothermal processes [7–12]. Therefore, a feasible synthesis of rutile nanostructures at low temperature is still an attractive target.

Recently, a new solvent system, room-temperature ionic liquids (ILs), has been developed and widely used as a new kind of reaction media owing to their intrinsic properties such as negligible vapor pressure, wide liquid temperature range, high thermal stability, large electrochemical window, and high ionic conductivity, etc. [13] Many inorganic nanostructures [14–16], including titanium dioxide [17–21], have been fabricated via various ILs-involved processes. For titania nanomaterials, however, few works about the synthesis of rutile nanostructures have been reported in ILs solution [9,22].

In this work, we report a facile method to prepare rutile films, in presence of IL, 1-butyl-3-methylimidazolium bromide ([Bmim]Br), under mild hydrothermal condition. Reaction time and the ratio of [Bmim]Br to $TiCl_4$ were varied to optimize the condition. Highly concentrated HCl was used to control the hydrolysis of $TiCl_4$ and enhance crystallization of rutile phase [22]. The rutile films were facilely deposited, which consisted of rectangular nanorods that arrayed against the glass substrates.

2. Experimental and characterization

2.1. Materials

[Bmim]Br was synthesized and purified according to previous literature [23]. Other reagents were AR grade from local commercial suppliers and used as accepted without further purification. Hydrochloric acid serves as an acidic catalyst to control hydrolysis rate of the titanium source.

* Corresponding authors at: Department of Material Chemistry, College of Chemistry, Nankai University, Tianjin 300071, China. Fax: +86 022 23502458.
E-mail addresses: pengpeng@zknu.edu.cn (P. Peng), zhwj@nankai.edu.cn (W. Zheng).

0022-4596/$ - see front matter © 2009 Published by Elsevier Inc.
doi:10.1016/j.jssc.2009.01.002

2.2. Synthesis of rutile films

The synthesis was conducted in a 6 mol dm^{-3} of HCl solution containing $TiCl_4$ and [Bmim]Br. The rutile nanorods films were typically prepared as follows. 2.0 g of [Bmim]Br and 0.2 mL of $TiCl_4$ was dissolved in 20 mL of HCl with vigorously stirring at 0 °C. Correspondingly, the molar ratio of [Bmim]Br to $TiCl_4$ is 500:1. Then, the solution was transferred to a Teflon-lined autoclave when the solution became clear. The glass substrate was previously coated by Degussa P25 nanoparticles, through dip coating from P25 suspension, before it was immersed in the solution. The reaction was carried out at 100 °C for 3, 8, and 12 h, respectively. After the reaction, the films, which were deposited on the substrate, were washed by deionized water and ethanol several times in turn, till pH value of filtrate was about 7, and then dried at 80 °C overnight.

2.3. Characterization

XRD measurement was performed on a Rigaku D/max 2500 diffractometer with Cu $K\alpha$ radiation ($\lambda = 0.154056$ nm) at 40 kV and 120 mA, using a nickel filter. SEM (scanning electron microscopy) was carried out by using Rigaku JEOL-6700F at 10 kV. TEM (transmission electron microscopy) and HRTEM images were recorded with a Tecnai G2 20 S-Twin transmission electron microscope operating at 200 kV. Raman spectra were measured in the frequency range 80–4000 cm^{-1} using Bruker RFS-100 FT-Raman spectrometer.

3. Result and discussion

3.1. Characterization of the films on seeded substrate

Typical SEM images of rutile nanorods films, deposited on seeded glass substrate for 3, 8, and 12 h are listed in Fig. 1. As shown by Fig. 1a, a large amount of small particles stick up against the substrate, and a few particles have presented rectangular shape by giving a careful observation, although others are still smoothly round on the tip. After 8 h deposition, the particles grow up towards rod shape against the substrate (Fig. 1b), most of which present obviously rectangular parallelepiped morphology. However, the width of the nanorods is not uniform but in a range from 30 to 350 nm. When the reaction time is prolonged to 12 h, the film made up of uniform nanorods is deposited. The low and high magnification images (Fig. 1c and d) give top images. The nanorods totally grow up with width of 100–200 nm, and the top presents regular squares. A cross-section image (Fig. 1e) reveals that the substrate is covered totally and continuously with the

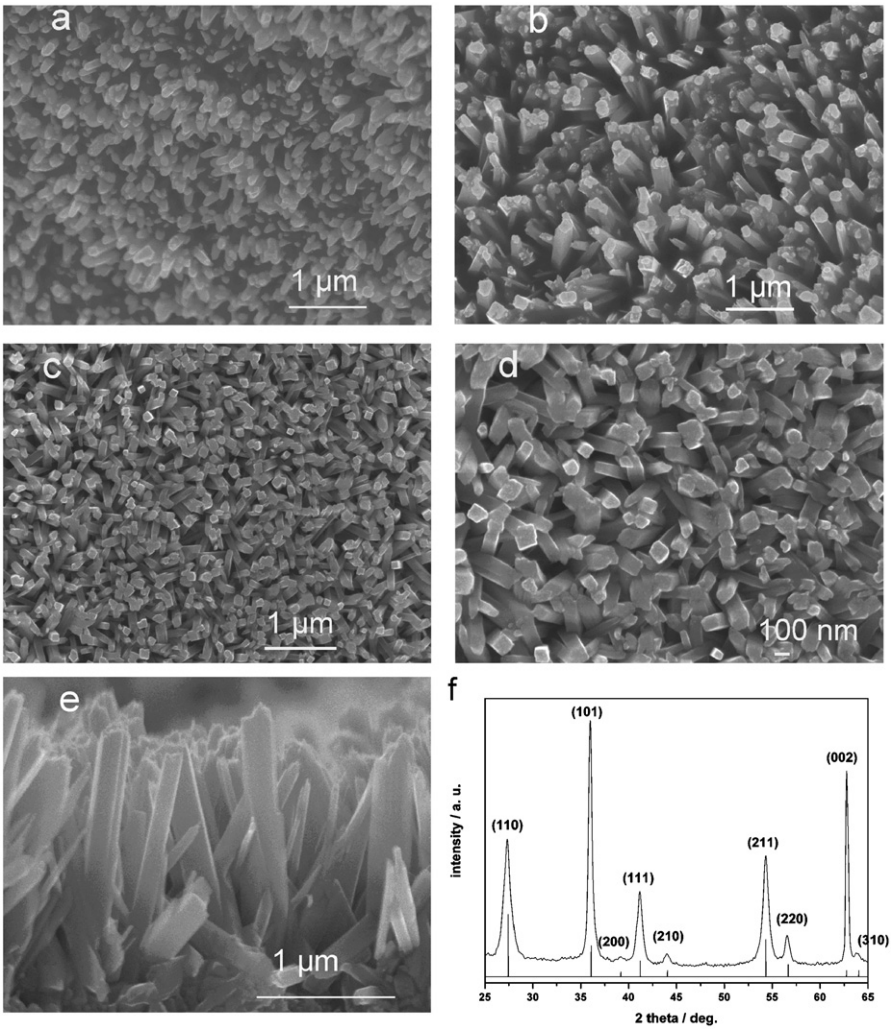

Fig. 1.

film and the length of the nanorods is more than 1 μm. Closer examination of the interface region shows that some nanorods initially inclined away from the substrate normal. The above description indicates that the nanorods grow up more and more uniformly towards regular rectangular shape when the reaction time is prolonged from 3 to 12 h. When the reaction time is excessively prolonged, however, the nanorods hardly continue growing. In addition, we find that the elevating temperatures have little effect on the size and shape of the nanorods and few rutile particles are formed when the temperature is lower than 100 °C, and on the other hand the [Bmim]Br is easy to decompose when the reaction temperature is over 180 °C in our synthesis.

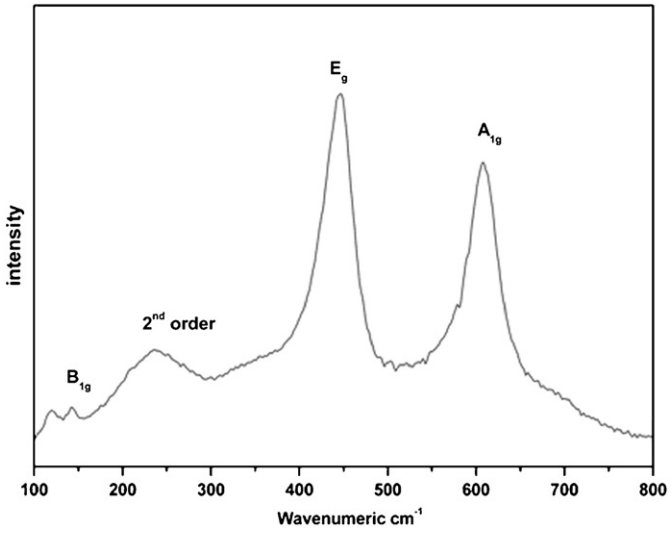

Fig. 2.

As confirmed by X-ray diffraction (XRD) (Fig. 1f), the film deposited for 12 h is identified with the pure rutile phase. All the diffraction peaks agree with those of TiO_2 in the rutile form (JCPDS no. 21-1276). No diffraction peak at 25° is detected, indicating anatase component of P25 can be dissolved in concentrated HCl and recrystallize to rutile via dissolution-crystallization process [24]. Furthermore, when considering that relative intensities of (101) and (002) peaks to (110) peak are, respectively, 59% and 14% in random rutile powders, remarkably enhanced (101) and (002) peaks indicate the nanorods are oriented against the substrate surface. The orientation observed in the XRD pattern reflects the growth direction of the rectangular nanorods, which is consistent with the observation of SEM images. Raman spectrum was also used to characterize the rutile nanorods film deposited for 12 h (Fig. 2). The vibration peaks in 143, 247, 443, and 612 cm^{-1} are detected, which are in good accordance with rutile four Raman active modes [25].

TEM images, shown in Fig. 3, give more structure informations of a single nanorod produced for 12 h. The results indicate the nanorod is not a integrated entity but a hierarchical structure. Two light lines along *c*-axis observed in a low magnification image (Fig. 3a, pointed out by white arrows) suggests the nanorod to split. Moreover, the corresponding high magnification image

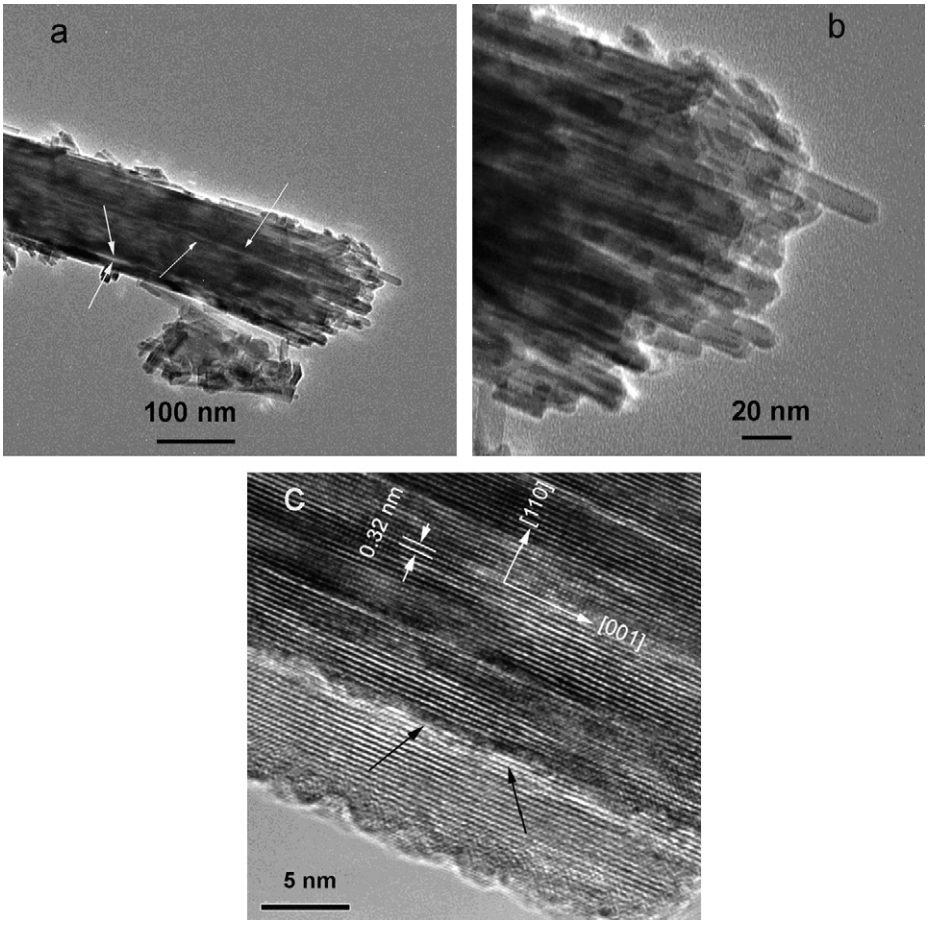

Fig. 3.

(Fig. 3b) reveals the gathering of rodlike crystals on the top. HRTEM measurement (Fig. 3c) determines the (110) and (001) planes by vertical interfacial angle and the d-spacing of 0.320 and 0.295 nm, respectively. So the growth pattern along *c*-axis is confirmed. The fringe of sub-nanorods is apparent in the image (pointed out by arrows). The growth process has made the rutile (110) surface to exhibit a dominant exposed plane (Fig. 3c). The predominant growth direction of [001] also agrees with the equilibrium shape of crystal in rutile phase [26].

3.2. Effect of P25 seeds

For comparison, a rutile film is directly deposited on non-seeded substrate in the same solution. The evolution of the films were monitored by SEM, similarly deposited for 3, 8, and 12 h (Fig. 4). Compared with the film on seeded substrate, few particles have been formed on bare substrate deposited for 3 h (Fig. 4a). It suggests that the presence of P25 seeds have accelerated the nucleation of the particles at the beginning of reaction. In Fig. 4b the nanorods are produced and oriented radially to form flower-like bundles, but their width and shape are similar to those obtained on seeded substrate. When deposited for 12 h, the film, consisting of nanorod flowers, was obtained with a certain extent discontinuity (Fig. 4c). The radial orientation of nanorods makes their long axis incline away from the substrate normal, which is similar to previous work [27]. The corresponding XRD pattern (Fig. 4d) reveals this kind of radial orientation on the substrate: the relative intensity of (002) peak has decreased to a normal degree, but the highest reflection (101) peak is still remained. It is confirmed that the predeposited P25 seeds facilitate the nucleation of the particles and array of the nanorods, but hardly change the crystal phase and growth pattern of the rod-like crystals.

3.3. Effect of [Bmim]Br on the films

In this system, the depositions are conducted by immersing non-seeded substrate in the solution with increasing ratio of [Bmim]Br to Ti: 0:1, 250:1, 750:1, 1250:1 and 2000:1. SEM measurement is used to monitor the effect of ILs on the films and the results obtained in various solution with increasing [Bmim]Br ratio are listed in Fig. 5. The microspheres are produced in absence of ILs (Fig. 5a). The rod-like particles are formed instead of microspheres when the [Bmim]Br is added (Fig. 5b and c). However, both size and yield of particles are decreased with increasing amount of the [Bmim]Br, till the substrate is only covered with small particles (Fig. 5e). We also tried increasing the ratio of [Bmim]Br to Ti over 2000 to prepared rutile films, but no particles were precipitated even at 150 °C for 24 h. It suggests that the excessive [Bmim]Br may hinder the continuous growth of the particles because the extended hydrogen may enhance the dissolution of Ti species via forming steady sol [28].

3.4. Formation mechanism

On the basis of the above discussion, the rod-like rutile monolayer films have been successfully fabricated in acidic IL-water system. In our synthetic route, high concentrated HCl (6 mol/mL) is used to control the hydrolysis of inorganic precursor. Furthermore, the HCl favor the formation of rutile phase, but cannot enhance the rod shape particles in the system (Fig. 5a). We attribute the formation of the large rod shape particles to the presence of [Bmim]Br. We believe that two particular properties of [Bmim]Br enhance the growth of rutile rods along *c*-axis. Firstly, as a kind of molten salts, [Bmim]Br ions promote the ionic strength by dissolving in solution, consequently enhance the solubility of Ti species. Secondly, although polar, [Bmim]Br can serve as traditional surfactant via dissolving in solution to form steady sol, and then cap on the crystal facets to enhance orientation of particles after rutile particles were precipitated [9]. However, It has been confirmed by above experiments that the excessive [Bmim]Br may hinder the precipitation of rutile particles from solution. Thus, the ratio of [Bmim]Br to Ti was fixed about 1000:1.

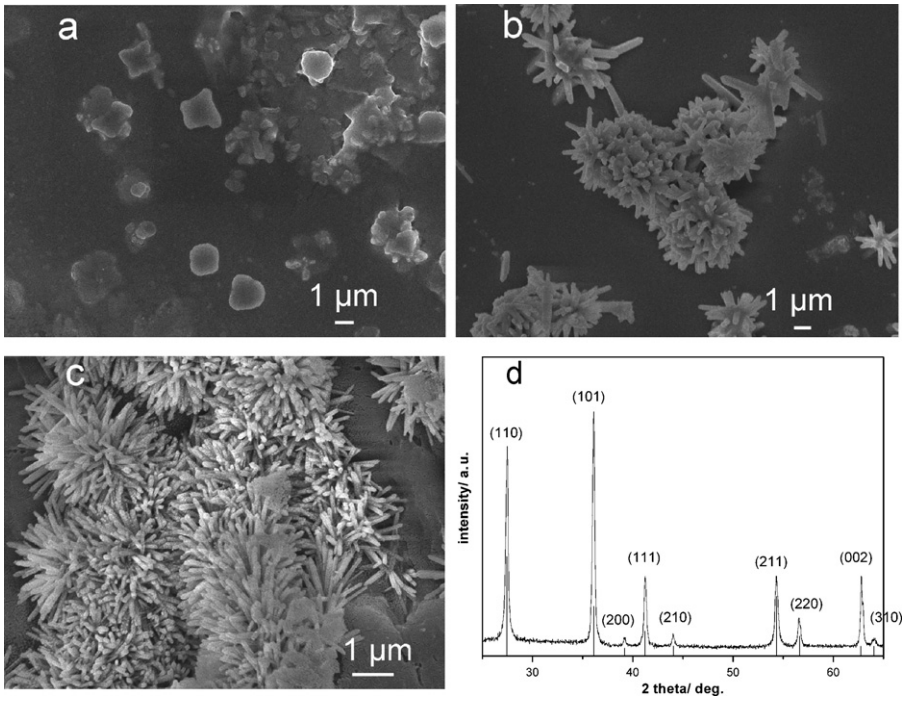

Fig. 4.

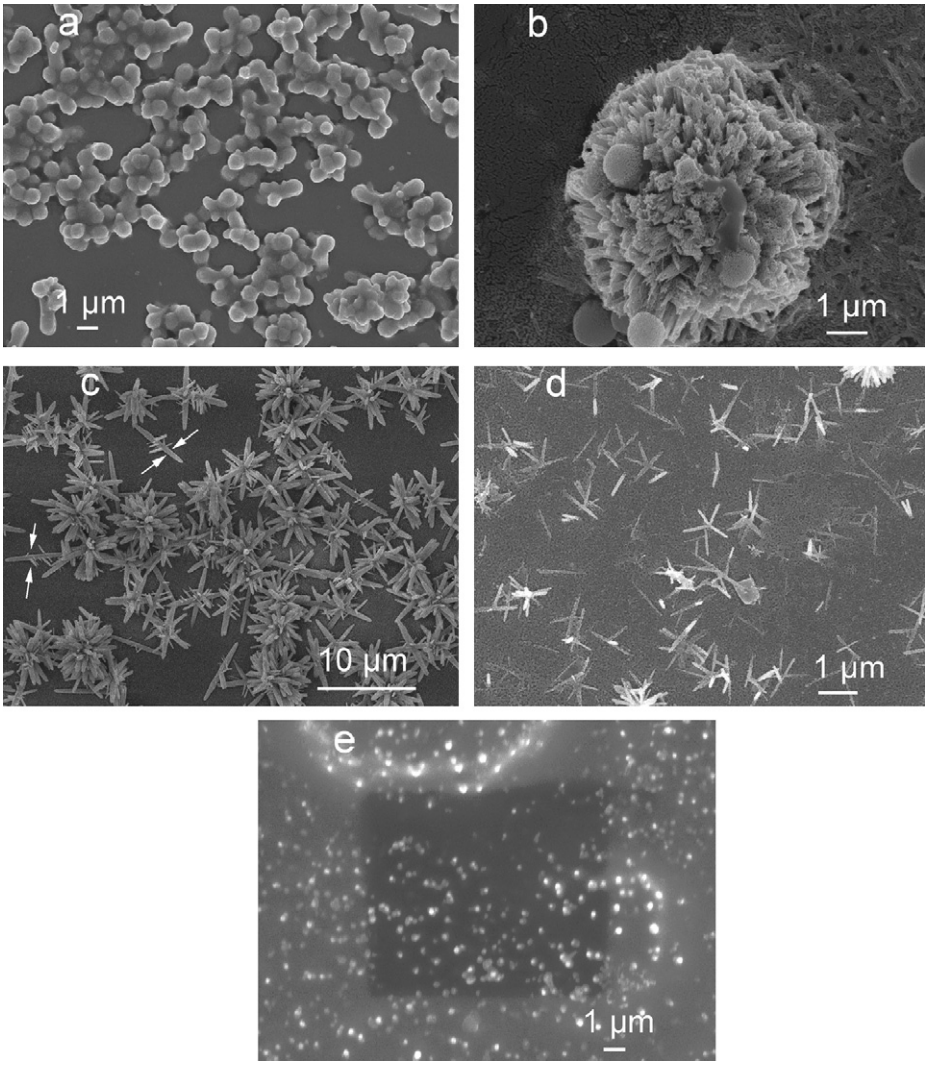

Fig. 5.

4. Conclusion

In summary, pure rutile films consisting of rectangular parallelepiped nanorods have been facilely deposited on the substrate in IL-water system. The presence of [Bmim]Br facilitate the growth of rod-like particles. The rod-like nanostructures of rutile are apparently different from previous results and can be rationally and reproducibly prepared in high yield, as well as on a large scale, according to this approach. We believe this approach may be developed to a general way to fabricate other nanostructures and further study is in progress.

Acknowledgments

We thank financial support of National Natural Science Foundation of China for this work (no. 20571044) and the Project Fundamental and Applied Research of Tianjin.

References

[1] J. Karch, R. Birriger, H. Gleiter, Nature 330 (1987) 556–558.
[2] M.R. Hoffmann, S.T. Martin, W. Choi, D.W. Bahnemann, Chem. Rev. 95 (1995) 69–96.
[3] M. Higuchi, K. Hatta, J. Takahashi, K. Kodaira, H. Kaneda, J. Saito, J. Cryst. Growth 208 (2000) 501–507.
[4] G.K.L. Goh, S.K. Donthu, P.K. Pallathadka, Chem. Mater. 16 (2004) 2857–2861.
[5] Y. Wang, L. Zhang, K. Deng, X. Chen, Z. Zou, J. Phys. Chem. C 111 (2007) 2709–2714.
[6] N.G. Park, G. Schlichthörl, J. van de Lagemaat, H.M. Cheong, A. Mascarenhas, A.J. Frank, J. Phys. Chem. B 103 (1999) 3308–3314.
[7] N.G. Park, J. van de Lagemaat, A.J. Frank, J. Phys. Chem. B 104 (2000) 8989–8994.
[8] T. Ohno, K. Tokieda, S. Higashida, M. Matsumura, Appl. Catal. A 244 (2003) 383–391.
[9] H. Kaper, F. Endres, I. Djerdj, M. Antonietti, B.M. Smarsly, J. Maier, Y.S. Hu, Small 3 (2007) 1753–1763.
[10] E. Hosono, S. Fujihara, K. Kakiuchi, H.J. Imai, Am. Chem. Soc. 126 (2004) 7790–7791.
[11] J.M. Wu, B. Qin, J. Am. Ceram. Soc. 90 (2007) 657–660.
[12] J.J. Wu, C.C. Yu, J. Phys. Chem. B 108 (2004) 3377–3379.
[13] M. Antonietti, D.B. Kuang, B. Smarsly, Y. Zhou, Angew. Chem. Int. Ed. 43 (2004) 4988–4992.
[14] Y.J. Zhu, W.W. Wang, R.J. Qi, X.L. Hu, Angew. Chem. Int. Ed. 43 (2004) 1410–1414.
[15] K. Yoo, H. Choi, D.D. Dionysiou, Chem. Commun. (2004) 2000–2001.
[16] E.R. Cooper, C.D. Andrews, P.S. Wheatley, P.B. Webb, P. Wormald, R.E. Morris, Nature 430 (2004) 1012–1016.
[17] Y. Zhou, M. Antonietti, J. Am. Chem. Soc. 125 (2003) 14960–14961.
[18] K.L. Ding, Z.J. Miao, Z.M. Liu, Z.F. Zhang, B.X. Han, G.M. An, S.D. Miao, Y.J. Xie, J. Am. Chem. Soc. 129 (2007) 6362–6363.
[19] K.S. Yoo, H. Choi, D.D. Dionysiou, Catal. Commun. 6 (2005) 259–262.
[20] Y. Liu, J. Li, M.J. Wang, Z.Y. Li, H.T. Liu, P. He, X.R. Yang, J.H. Li, Cryst. Growth Des. 5 (2005) 1643–1649.
[21] T. Nakashima, N. Kimizuka, J. Am. Chem. Soc. 125 (2003) 6386–6387.
[22] N. Yu, L. Gong, H. Song, Y. Liu, D. Yin, J. Solid State Chem. 180 (2007) 799–803.

[23] J.G. Huddleston, A.E. Visser, W.M. Reichert, H.D. Willauer, G.A. Broker, R.D. Rogers, Green Chem. 3 (2001) 156–164.
[24] M. Wu, G. Lin, D. Chen, G. Wang, D. He, S. Feng, R. Xu, Chem. Mater. 14 (2002) 1974–1980.
[25] S. Kelly, F.H. Pollak, M. Tomkiewicz, J. Phys. Chem. B 101 (1997) 2730–2734.
[26] Y.Q. Zheng, E.W. Shi, Z.Z. Chen, W.J. Li, X.F. Hu, J. Mater. Chem. 11 (2001) 1547–1551.
[27] G.K.L. Goh, X.Q. Han, C.P.K. Liew, C.S.S. Tay, J. Electrochem. Soc. 152 (2005) C532–C536.
[28] K. Dong, S. Zhang, D. Wang, X. Yao, J. Phys. Chem. A 110 (2006) 9775–9782.